DOI 10.1007/s10593-020-02647-y

Chemistry of Heterocyclic Compounds **2020**, *56*(2), 219–225

Synthesis and spectral properties of carbazole-coumarin hybrid dyes

Shengling Li[1], Duanlin Cao[1], Zhiyong Hu[1,2], Zhichun Li[1], Xianjiao Meng[1], Xinghua Han[1,2], Wenbing Ma[1,2]*

[1] *School of Chemical Engineering and Technology, North University of China, Taiyuan 030051, China; e-mail: 1344729066@qq.com*

[2] *National Demonstration Center for Experimental Comprehensive Chemical Engineering Education, North University of China, Taiyuan 030051, China; e-mail: mawenbing@nuc.edu.cn*

Published in Khimiya Geterotsiklicheskikh Soedinenii, 2020, *56*(2), 219–225

Submitted June 14, 2019
Accepted after revision November 14, 2019

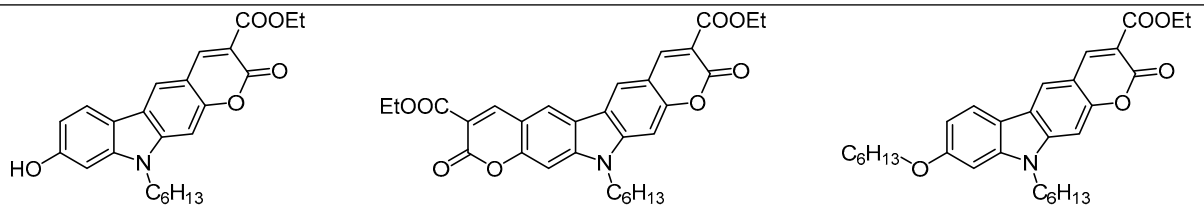

In this study, three carbazole-coumarin hybrid dyes were successfully synthesized, and their UV-vis absorption spectra, fluorescence spectra, and structural properties were investigated. The results indicated that diethyl 12-hexyl-2,9-dioxo-9,12-dihydro-2*H*-dipyrano[2,3-*b*:3',2'-*h*]-carbazole-3,8-dicarboxylate showed a slight red shift of the maximum absorption wavelength, and its fluorescence intensity was above 4000 arb units, about 22 times higher than that of ethyl 10-hexyl-8-hydroxy-2-oxo-2,10-dihydropyrano[2,3-*b*]carbazole-3-carboxylate and ethyl 10-hexyl-8-(hexyloxy)-2-oxo-2,10-dihydropyrano[2,3-*b*]carbazole-3-carboxylate in $CHCl_3$. The fluorescence intensity of the three compounds first increases and then decreases with the rise of concentration, and the maximum emission wavelength shows a slight red shift. The stability pH range of diethyl 12-hexyl-2,9-dioxo-9,12-dihydro-2*H*-dipyrano[2,3-*b*:3',2'-*h*]carbazole-3,8-dicarboxylate in THF was 2–10.

Keywords: carbazole, coumarin, fluorescent dye, Knoevenagel reaction, spectral properties.

Carbazole and its derivatives are widely used in supramolecular recognition,[1–3] photoelectric materials,[4–6] pharmaceutics,[7,8] chemosensors,[9–12] dyes,[13–15] and in other fields due to their advantages of large conjugated systems, strong electron-transfer ability, high thermal and photochemical stability, and abundant active sites. Carbazole-based fluorescent dyes are of particular research interest on account of their simple synthesis and highly planar structure. However, their applications can be limited by the low fluorescence intensity and short excitation wavelength, which highlights the need to optimize the carbazole structure. Carbazole is a typical electron donor commonly used in D–π–A,[16–19] D–π–A–π–D,[20–22] A–π–D–π–A,[23] and A–π–D–D–π–A[24] structures. For structural modification, usually, functional groups are introduced into 3, 6, and 9 positions of carbazole, giving compounds with many unique properties and biological activities.[25,26] For instance, Schiff base,[27,28] double bond,[22,29] or triple bond[30] are introduced into 3, 6 or 2, 7 positions of carbazole to increase the conjugated chain length. Fluorescent groups such as spiropyran,[31] rhodamine,[32] BODIPY,[33,34] and coumarin[35] can also be introduced in an indirect way to expand the conjugated system and enhance the intramolecular electron-transfer ability. Coumarin fluorophores are often used in structural design of fluorescent dyes due to their high fluorescence quantum yield, large Stokes shift, and good light stability.[36,37] However, carbazole core is rarely used as a part of the parent structure for the synthesis of coumarin derivatives.

In this study, three novel carbazole-coumarin derivatives ethyl 10-hexyl-8-hydroxy-2-oxo-2,10-dihydropyrano[2,3-*b*]-carbazole-3-carboxylate (**CC**), diethyl 12-hexyl-2,9-dioxo-9,12-dihydro-2*H*-dipyrano[2,3-*b*:3',2'-*h*]carbazole-3,8-dicarboxylate (**DCC**), and ethyl 10-hexyl-8-(hexyloxy)-2-oxo-2,10-dihydropyrano[2,3-*b*]carbazole-3-carboxylate (**HCC**) were synthesized by a series of reactions such as methoxylation, formylation, and Knoevenagel condensation, and their spectral and structural characteristics under different pH conditions were investigated. The results of this study would provide some insights into the design and preparation of new carbazole derivatives.

The molecular structures and synthetic routes are shown in Scheme 1. 2,7-Dibromo-9-hexyl-9*H*-carbazole (**1**) was

Scheme 1

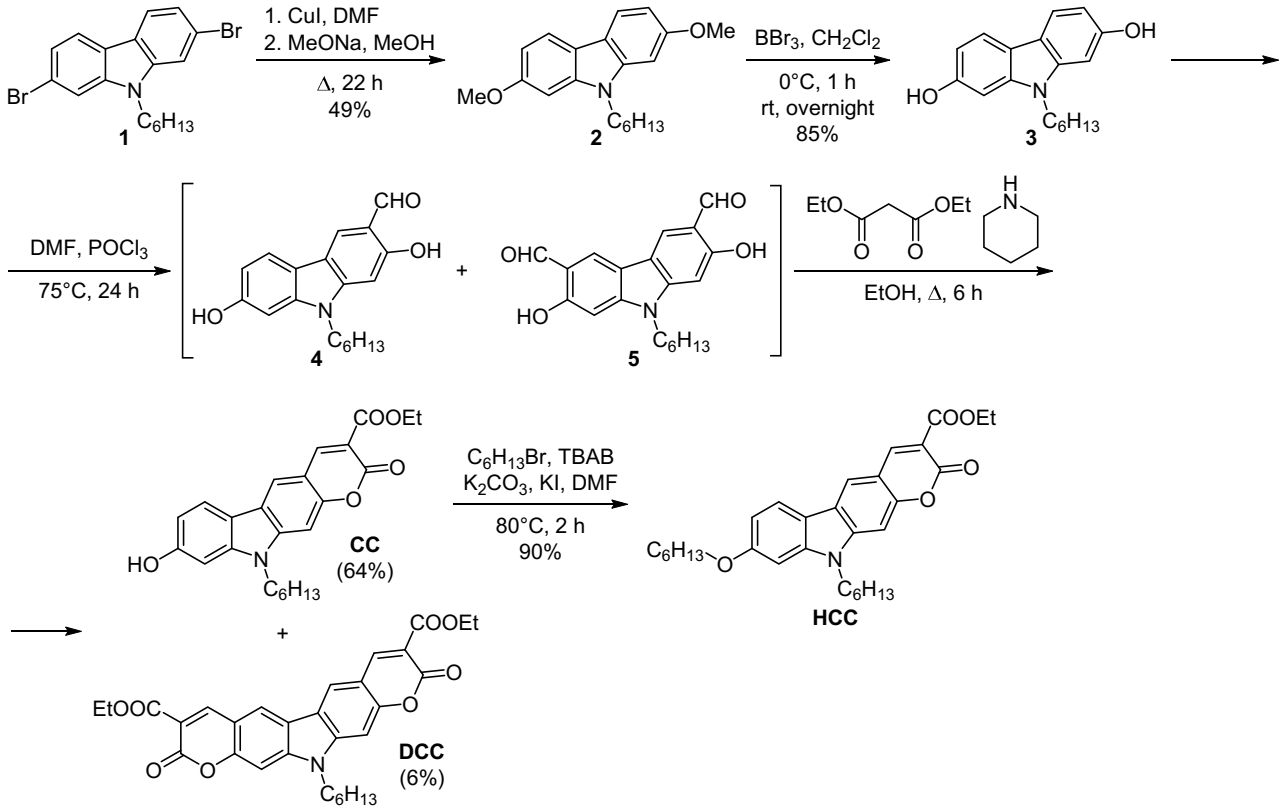

synthesized as described in a previous study.[38] Compound **2** was synthesized using methoxylation with MeONa and CuI in 49% yield, then compound **3** was prepared by demethylation with BBr_3 in high yield (85%). Compound **3** was then subjected to a Vilsmeier–Haack formylation reaction to obtain the intermediate compounds **4** and **5**. Since products **4** and **5** have similar polarity and could not be separated under the existing laboratory conditions, they were used directly in the next step without further separation and purification. Compounds **CC** and **DCC** were synthesized by Knoevenagel condensation and easily separated by column chromatography as the difference in R_f values was 0.4. Finally, compound **HCC** was synthesized in a reaction with 1-bromohexane in DMF and anhydrous K_2CO_3 in good yield. All synthesized compounds were characterized by ^1H, ^{13}C NMR and HRMS (see the Supplementary information file, Figs. S1–S15).

UV-vis absorption of compounds **CC**, **DCC**, and **HCC** was investigated in different solvents. Compound **CC** showed two obvious absorption bands in the absorption spectra (Fig. 1). The absorption band at 325 nm was assigned to the localized transition of carbazole, while that at 350–450 nm was assigned to the delocalized π–π* transition of coumarin moiety. The maximum absorption wavelength of compound **CC** in the nine solvents ranged from 388 to 399 nm. The highest absorbance of compound **CC** was observed in CH_2Cl_2 and $CHCl_3$. Notably, the lowest absorbance and the lowest maximum absorption wavelength of compound **CC** were observed in *n*-hexane. Compared to the solutions of compound **CC** in other solvents, solution in *n*-hexane showed a slight red shift of the maximum absorption wavelength.

Compound **HCC** also had two strong absorption peaks at around 325 and 400 nm (Fig. 2). However, the change of solvent polarity resulted in a slight shift of the maximum absorption wavelength. Compound **HCC** showed a more obvious blue shift in *n*-hexane compared to other solvents.

Compound **DCC** had two absorption peaks with the maximum absorption wavelength higher than 400 nm (Fig. 3). However, compared to compound **CC** and **HCC**, the

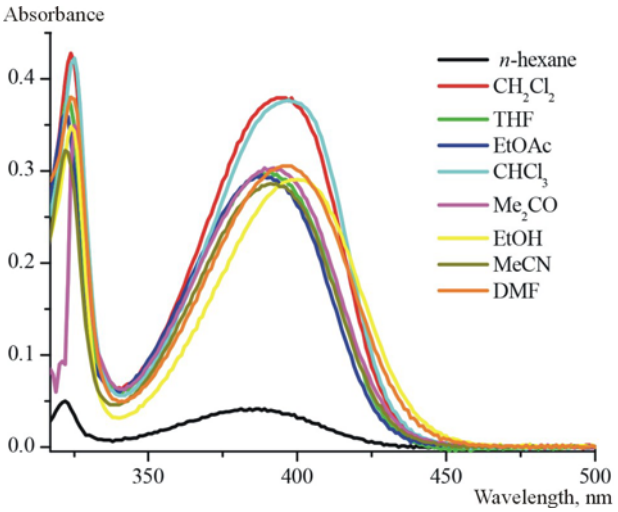

Figure 1. UV-vis absorption of compound **CC** ($1 \cdot 10^{-5}$ mol/l) in *n*-hexane, CH_2Cl_2, THF, EtOAc, $CHCl_3$, Me_2CO, EtOH, MeCN, and DMF.

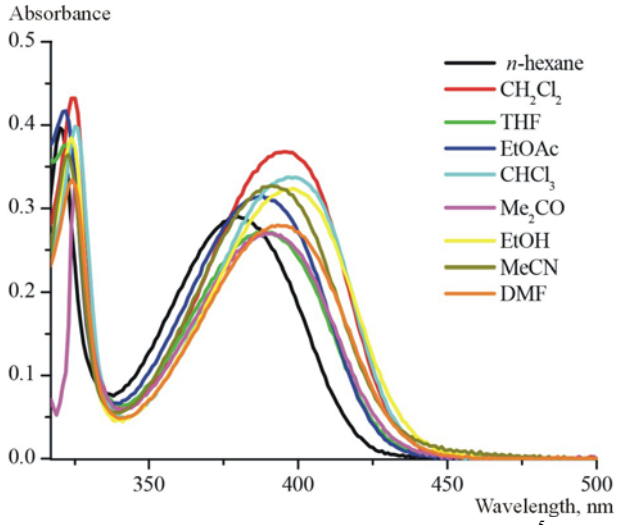

Figure 2. UV-vis absorption of compound **HCC** ($1 \cdot 10^{-5}$ mol/l) in *n*-hexane, CH_2Cl_2, THF, EtOAc, $CHCl_3$, Me_2CO, EtOH, MeCN, and DMF.

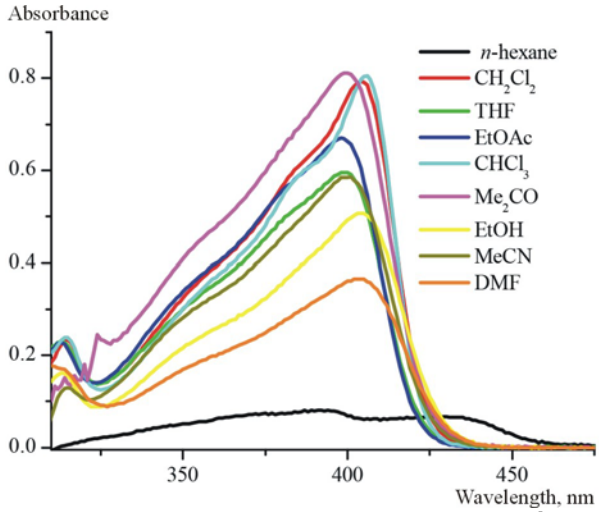

Figure 3. UV-vis absorption of compound **DCC** ($1 \cdot 10^{-5}$ mol/l) in *n*-hexane, CH_2Cl_2, THF, EtOAc, $CHCl_3$, Me_2CO, EtOH, MeCN, and DMF.

intensity of the absorption at around 325 nm was significantly reduced, and the absorption peak even disappeared in *n*-hexane. However, the intensity of the absorption peak at around 400 nm was doubled, and the maximum absorption wavelength was slightly red-shifted.

Fluorescence intensity of compounds **CC**, **DCC**, and **HCC** was measured in the same solvents as absorbance. The maximum emission wavelength of compound **CC** was 468 nm in *n*-hexane and above 500 nm in other solvents (Fig. 4). Compound **CC** showed highest fluorescence intensity in THF, EtOAc, and $CHCl_3$. The fluorescence intensity of compound **HCC** in THF, EtOAc, and $CHCl_3$ was relatively higher compared to compound **CC**, and the emission wavelength was above 500 nm (Fig. 5). The maximum fluorescence intensity of compound **HCC** was observed in *n*-hexane (213 arb units), and the emission maximum wavelength was 453 nm (Table 1).

The fluorescence intensity of compound **DCC** in $CHCl_3$ was over 4000 arb units (Fig. 6), and it was higher than that of compounds **CC** and **HCC** with the same concentration in $CHCl_3$, probably due to modification of carbazole core with coumarin cycles on both sides making molecular structure highly symmetrical. The coumarin lactone ring, as the electron acceptor, absorbed electrons from the carbazole conjugated system, resulting in an increase in electron transmission capacity of the molecular structure and consequently in an increase in fluorescence. Compound **HCC** had higher absorbance and fluorescence intensity in *n*-hexane than compounds **CC** and **DCC**, mainly because the introduction of the alkyl chain to compound **HCC** prevented the aggregation effect and increased the solubility and electron-donating properties of the compound.

We compared the spectral properties of the three synthesized compounds with carbazole and coumarin in

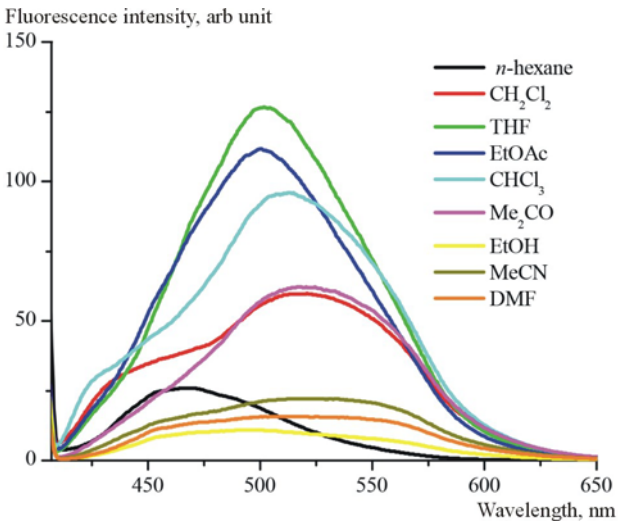

Figure 4. Fluorescence spectra of compound **CC** ($1 \cdot 10^{-5}$ mol/l) in *n*-hexane, CH_2Cl_2, THF, EtOAc, $CHCl_3$, Me_2CO, EtOH, MeCN, and DMF at an excitation of 399 nm.

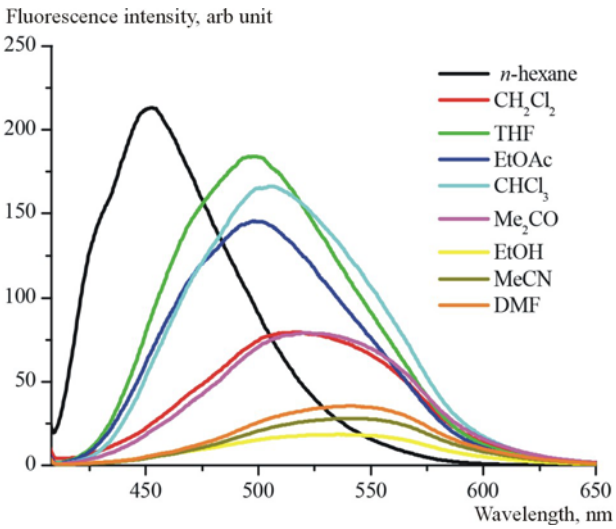

Figure 5. Fluorescence spectra of compound **HCC** ($1 \cdot 10^{-5}$ mol/l) in *n*-hexane, CH_2Cl_2, THF, EtOAc, $CHCl_3$, Me_2CO, EtOH, MeCN, and DMF at an excitation of 399 nm.

Table 1. Spectral data of carbazole, ethyl 2-oxo-2*H*-chromene-3-carboxylate, compounds **CC**, **DCC**, and **HCC** at concentration $1 \cdot 10^{-5}$ mol/l

Compound	Solvent	λ_{max}, nm	$\varepsilon \cdot 10^4$, $l \cdot mol^{-1} \cdot cm^{-1}$	λ_{em}, nm	FI, arb unit	Stokes shift, cm^{-1}
Carbazole	DMSO	292	0.82	359	51.57	6391
Ethyl 2-oxo-2*H*-chromene-3-carboxylate	EtOH	292	0.49	418	25.65	10323
CC	*n*-Hexane	389	0.41	468	26.07	4339
CC	CH_2Cl_2	399	3.79	521	59.94	5867
CC	THF	391	3.12	501	126.8	5615
CC	EtOAc	388	2.91	500	111.8	5773
CC	$CHCl_3$	397	3.77	513	95.98	5696
CC	Me_2CO	392	3.04	516	62.28	6130
CC	EtOH	398	2.80	499	11.05	5086
CC	MeCN	391	2.79	520	22.19	6345
CC	DMF	398	3.04	516	15.82	5746
DCC	*n*-Hexane	394	0.87	458	151.5	3547
DCC	CH_2Cl_2	404	7.99	439	3118	1973
DCC	THF	398	5.99	438	2275	2295
DCC	EtOAc	398	6.66	437	2828	2242
DCC	$CHCl_3$	406	8.05	428	4053	1266
DCC	Me_2CO	400	8.13	461	1789	3308
DCC	EtOH	405	4.96	483	1592	3987
DCC	MeCN	401	5.80	467	1447	3524
DCC	DMF	404	3.64	469	1476	3431
HCC	*n*-Hexane	380	2.90	453	213.4	4241
HCC	CH_2Cl_2	395	3.71	517	79.80	5974
HCC	THF	388	2.72	498	184.2	5693
HCC	EtOAc	388	3.15	498	145.5	5693
HCC	$CHCl_3$	399	3.37	505	166.5	5261
HCC	Me_2CO	389	2.72	520	79.30	6476
HCC	EtOH	398	3.20	535	18.46	6434
HCC	MeCN	391	3.33	543	28.03	7159
HCC	DMF	393	2.79	541	35.60	6961

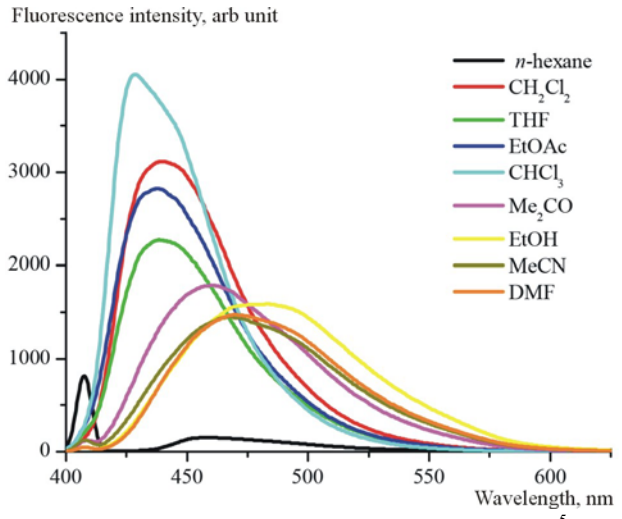

Figure 6. Fluorescence spectra of compound **DCC** ($1 \cdot 10^{-5}$ mol/l) in *n*-hexane, CH_2Cl_2, THF, EtOAc, $CHCl_3$, Me_2CO, EtOH, MeCN, and DMF at an excitation of 406 nm.

solution. The results showed that compound **DCC** had better spectral properties, such as higher molar extinction coefficients and stronger fluorescence intensity. The relevant spectral data are shown in Table 1.

Fluorescence self-quenching tests of compounds **CC**, **DCC**, and **HCC** were performed in THF. As the solution concentration increased, the fluorescence intensity of the three compounds first increased and then decreased and the maximum emission wavelength showed a slight red shift, and the maximal fluorescence intensities of compounds **CC**, **HCC**, and **DCC** were observed at $4 \cdot 10^{-5}$, $4 \cdot 10^{-5}$, and $1 \cdot 10^{-5}$ mol/l, respectively (Figs. 7–9). Probably, in the case of high concentration, intermolecular aggregation and the probability of collision between fluorescent molecules was larger, resulting in a large energy loss and causing fluorescence self-quenching phenomenon.

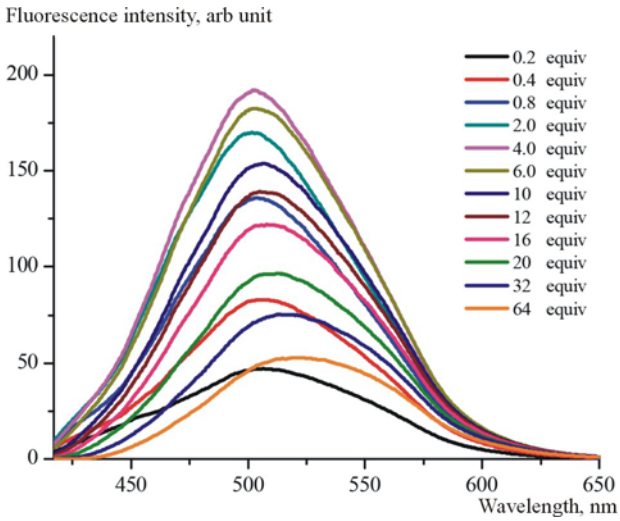

Figure 7. Fluorescence self-quenching test of compound **CC** at various concentrations (0.2, 0.4, 0.8, 2.0, 4.0, 6.0, 10, 12, 16, 20, 32, and 64 equiv to $1 \cdot 10^{-5}$ mol/l) at an excitation of 399 nm in THF.

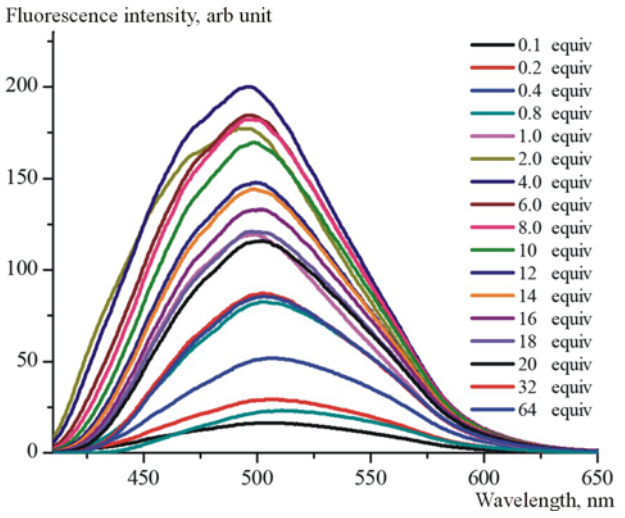

Figure 8. Fluorescence self-quenching test of compound **HCC** at various concentrations (0.1, 0.2, 0.4, 0.8, 1.0, 2.0, 4.0, 6.0, 8.0, 10, 12, 14, 16, 18, 20, 32, and 64 equiv to $1 \cdot 10^{-5}$ mol/l) at an excitation of 399 nm in THF.

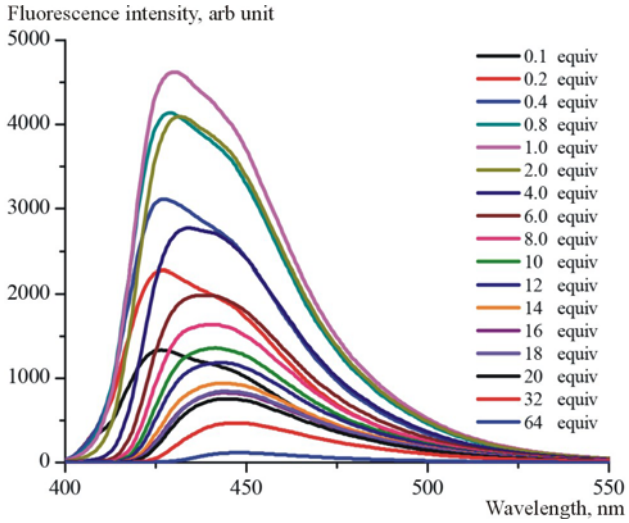

Figure 9. Fluorescence self-quenching test of compound **DCC** at various concentrations (0.1, 0.2, 0.4, 0.8, 1.0, 2.0, 4.0, 6.0, 8.0, 10, 12, 14, 16, 18, 20, 32, and 64 equiv to $1 \cdot 10^{-5}$ mol/l) at an excitation of 406 nm in $CHCl_3$.

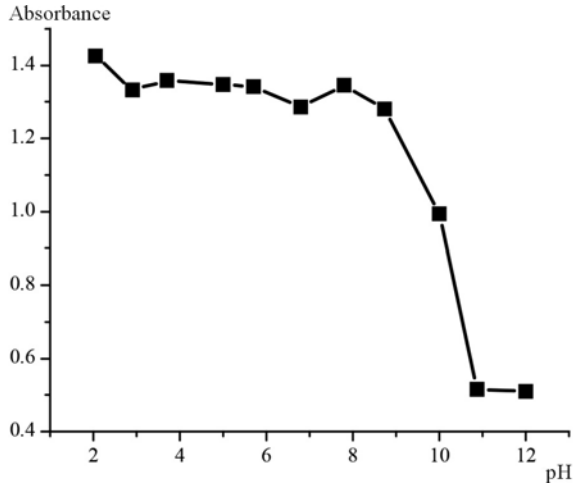

Figure 10. UV-vis absorption of compound **DCC** in THF solutions ($1 \cdot 10^{-5}$ mol/l), pH value 2–12.

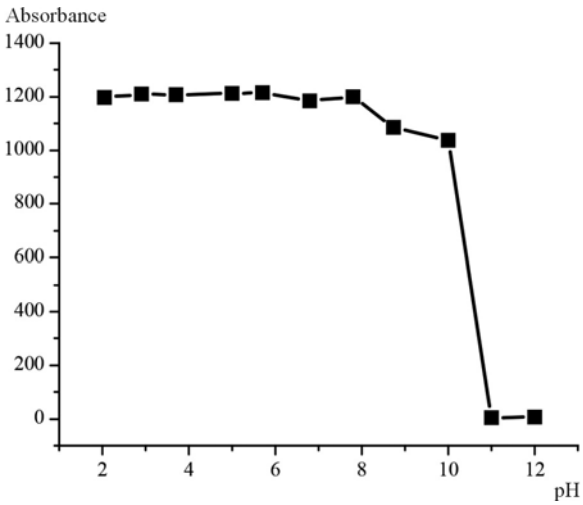

Figure 11. Fluorescence intensity dependence of compound **DCC** in THF solutions ($1 \cdot 10^{-5}$ mol/l), pH value 2–12.

The maximum absorption wavelength of compounds **CC** and **HCC** was below 400 nm, while that of compound **DCC** was above 400 nm with high absorbance (Table 1), the relevant spectral data are shown in Table 1. This might be because two coumarin lactone rings were directly connected to the carbazole, leading to an increase in the conjugation of the whole molecule and consequently stronger electron transport capacity and higher fluorescence.

The maximum emission wavelength of compounds **CC** and **HCC** was around 510 nm, and the fluorescence intensity was within 213 arb units (Table 1). However, the maximum emission wavelength of compound **DCC** was around 425 nm, and the fluorescence intensity was over 4000 arb units. The relevant spectral data are shown in Table 1. As the molecular conjugation increased, the electron transport capacity became stronger, and the maximum absorption wavelength was red-shifted. According to the photon energy formula $\Delta E = hc(1/\lambda_{ex} - 1/\lambda_{em})$, $\Delta\lambda$ is proportional to ΔE, so the shorter the emission wavelength, the lower the energy required. It could be seen from the spectrum that compound **DCC** had the longest absorption wavelength, the shortest emission wavelength, and the strongest fluorescence intensity.

The effect of pH was investigated on compound **DCC** in THF solutions. The absorbance tended to be stable at pH 2–9, and decreased in strongly alkaline solutions. Fluorescence intensity of compound **DCC** was stable in the pH range of 2–10, but it decreased significantly at pH 10–12, which could be attributed to the destruction of the compound under strong alkali conditions (Figs. 10 and 11).

In summary, three carbazole-coumarin compounds containing a large conjugated system were successfully synthesized and were characterized by ^{1}H, ^{13}C NMR and ESI-HRMS. The results showed that the maximum absorption wavelength of the three compounds increased with the increase of solvent polarity. However, diethyl 12-hexyl-2,9-dioxo-9,12-dihydro-2*H*-dipyrano[2,3-*b*:3',2'-*h*]-carbazole-3,8-dicarboxylate showed a slight red shift of the maximum absorption wavelength, and its fluorescence intensity was about 22 times higher than that of ethyl 10-hexyl-8-hydroxy-2-oxo-2,10-dihydropyrano[2,3-*b*]-carbazole-3-carboxylate and ethyl 10-hexyl-8-(hexyloxy)-2-oxo-2,10-dihydropyrano[2,3-*b*]carbazole-3-carboxylate. The fluorescence intensity of the three compounds first increased and then decreased with the rise of concentration, and the maximum emission wavelength showed a slight red shift. The fluorescence intensity of diethyl 12-hexyl-2,9-dioxo-9,12-dihydro-2*H*-dipyrano[2,3-*b*:3',2'-*h*]carbazole-3,8-dicarboxylate in THF was stable in the pH range of 2–10, but it decreased significantly at pH 10–12.

Experimental

^{1}H and ^{13}C NMR spectra (400 and 100 MHz, respectively) were recorded on a Bruker Avance III spectrometer in $CDCl_3$, DMSO-d_6, or Me_2CO-d_6 solution with TMS as internal standard at 25°C. HRMS (ESI) spectra were recorded on a Bruker Solarix XR Fourier transform-ion cyclotron resonance (FT-ICR) mass spectrometer. Melting

points were measured on a WRS-C1 digital melting-point apparatus. The pH of all solutions was adjusted on a PHS-3C pH meter. The pH was set using aqueous solutions of NaOH (1 mol/l) and HCl (1 mol/l) for 11 distinct solutions of compound **DCC** in THF. UV spectra of all samples were recorded on a UV-2602 spectrophotometer, and all fluorescence spectra were recorded on a HITACHI F-2500 spectrophotometer. Fluorescence spectra in different solvents were recorded at an excitation wavelength 399 nm for compounds **CC** and **HCC** and 406 nm for compound **DCC**. Except for fluorescence self-quenching experiments, the concentrations of other test samples were $1 \cdot 10^{-5}$ mol/l. The slits of emission and excitation were 5 nm in all experiments. Column chromatography was accomplished using 45–75 μm silica gel from Qingdao Ocean Chemical Co., Ltd.

The solvents and materials were purchased from Aladdin and Energy Chemical Reagents Ltd.

9-Hexyl-2,7-dimethoxy-9*H*-carbazole (2). A mixture of 2,7-dibromo-9-hexyl-9*H*-carbazole (**1**) (920 mg, 2.3 mmol), CuI (1.7 g, 8.9 mmol), and dry DMF (2 ml) was stirred at room temperature for 10 min. Then, MeONa solution in MeOH (5.4 mol/l, 12.8 ml, 7.8 mmol) was added dropwise to the mixture and it turned yellow-green, the mixture was heated under reflux for 22 h. After that, the mixture was cooled to room temperature, precipitate was filtered off, filter cake was washed with EtOAc. Filtrate was concentrated under reduced pressure, and the residue was purified by column chromatography on silica gel, eluent petroleum ether – EtOAc, 30:1. Yield 340 mg (49%), white crystals, mp 73.9–74.3°C. ^{1}H NMR spectrum (Me_2CO-d_6), δ, ppm (*J*, Hz): 7.89 (2H, d, *J* = 8.4, H Ar); 7.06 (2H, d, *J* = 2.0, H Ar); 6.80 (2H, dd, *J* = 8.4, *J* = 2.4, H Ar); 4.35 (2H, t, *J* = 7.2, $NC\underline{H}_2CH_2$); 3.90 (6H, s, $2OCH_3$); 1.91–1.83 (2H, m, $NCH_2C\underline{H}_2$); 1.46–1.25 (6H, m, $CH_2CH_2CH_2$); 0.87 (3H, t, *J* = 6.8, CH_3). ^{13}C NMR spectrum (DMSO-d_6), δ, ppm: 158.2; 141.9; 120.5; 116.5; 107.5; 94.1; 55.9; 42.5; 31.5; 28.6; 26.5; 22.5; 14.3. Found, *m*/*z*: 312.1958 $[M+H]^+$. $C_{20}H_{26}NO_2$. Calculated, *m*/*z*: 312.1958.

9-Hexyl-9*H*-carbazole-2,7-diol (3). BBr_3 (3.9 g, 15.4 mmol) was slowly dropped into a cold (0°C) solution of 9-hexyl-2,7-dimethoxy-9*H*-carbazole (**2**) (2.0 g, 6.4 mmol) in dry CH_2Cl_2 (40 ml) under Ar atmosphere, and stirred at 0°C for 1 h, then overnight at room temperature. Distilled H_2O was added dropwise to the solution to quench the reaction, and the solution was extracted with EtOAc. The solvent was removed under reduced pressure to give a gummy mass, which was purified by silica gel column chromatography, eluent petroleum ether – EtOAc, 1:1. Yield 1.6 g (85%), white powder, mp >183.9°C (decomp.). ^{1}H NMR spectrum (DMSO-d_6), δ, ppm (*J*, Hz): 9.29 (2H, s, OH); 7.70 (2H, d, *J* = 8.0, H Ar); 6.78 (2H, d, *J* = 2.0, H Ar); 6.60 (2H, dd, *J* = 8.4, *J* = 2.0, H Ar); 4.12 (2H, t, *J* = 6.8, $NC\underline{H}_2CH_2$); 1.70 (2H, t, *J* = 6.8, $NCH_2C\underline{H}_2$); 1.31–1.22 (6H, m, $CH_2CH_2CH_2$); 0.84 (3H, t, *J* = 6.8, CH_3). ^{13}C NMR spectrum (DMSO-d_6), δ, ppm: 155.8; 142.0; 120.1; 115.8; 108.2; 95.4; 42.6; 31.5; 28.6; 26.7; 22.5; 14.4. Found, *m*/*z*: 284.1645 $[M+H]^+$. $C_{18}H_{22}NO_2$. Calculated, *m*/*z*: 284.1645.

Intermediates 4 and 5. A 50-ml three-necked flask containing anhydrous DMF (2.8 ml 36.4 mmol) was cooled to below 0°C under Ar atmosphere. Distilled phosphorous oxychloride (3.7 ml, 39.7 mmol) was added dropwise to the contents of the flask, and the mixture was first stirred for 1 h at 0°C and then for another 2 h at room temperature. 9-Hexyl-9*H*-carbazole-2,7-diol (**3**) (0.4 g, 1.4 mmol) in DMF (3 ml) was added dropwise to the above solution, and then the reaction mixture was heated at 75°C for 24 h. The solution was cooled to room temperature, poured into ice water, stirred for 0.5 h, and neutralized to pH 7–8 by dropwise addition of 4 M NaOH aqueous solution. The mixture was extracted with EtOAc, and the solvent was removed under reduced pressure to give a gummy mass which was used directly in the next procedure.

Ethyl 10-hexyl-8-hydroxy-2-oxo-2,10-dihydropyrano-[2,3-*b*]carbazole-3-carboxylate (CC) and diethyl 12-hexyl-2,9-dioxo-9,12-dihydro-2*H*-dipyrano[2,3-*b*:3',2'-*h*]carbazole-3,8-dicarboxylate (DCC). A 100-ml round-bottom flask containing the above yellow solid (200 mg), piperidine (240 μl, 2.6 mmol), diethyl malonate (770 mg, 720 μl, 4.8 mmol), and absolute EtOH (10 ml) was heated under reflux for 6 h and monitored by TLC. The mixture was cooled to room temperature, filtered, the filter cake was washed with cold EtOH and purified by silica gel column chromatography, eluent CH_2Cl_2–CH_3OH, 200:1.

Ethyl 10-hexyl-8-hydroxy-2-oxo-2,10-dihydropyrano-[2,3-*b*]carbazole-3-carboxylate (CC). Yield 181 mg (64%, two-step total yield), yellow solid, mp >238.6°C (decomp.). ^{1}H NMR spectrum (DMSO-d_6), δ, ppm (*J*, Hz): 9.81 (1H, s, OH); 8.85 (1H, s, H Ar); 8.47 (1H, s, H Ar); 7.93 (1H, d, *J* = 8.0, H Ar); 7.59 (1H, s, H Ar); 6.94 (1H, d, *J* = 2.0, H Ar); 6.78 (1H, dd, *J* = 8.4, *J* = 2.0, H Ar); 4.33–4.27 (4H, m, $NC\underline{H}_2CH_2$, $COOC\underline{H}_2CH_3$); 1.77–1.70 (2H, m, $NCH_2C\underline{H}_2$); 1.33 (3H, t, *J* = 7.2, $COOCH_2C\underline{H}_3$); 1.30–1.21 (6H, m, $CH_2CH_2CH_2$); 0.82 (3H, t, *J* = 6.8, CH_3). ^{13}C NMR spectrum (DMSO-d_6), δ, ppm: 163.6; 158.2; 157.3; 153.7; 150.9; 144.9; 143.6; 122.0; 121.7; 121.1; 114.4; 112.2; 110.9; 110.2; 96.5; 95.9; 61.3; 43.1; 31.4; 28.4; 26.5; 22.5; 14.6; 14.3. Found, *m*/*z*: 408.1806 $[M+H]^+$. $C_{24}H_{26}NO_5$. Calculated, *m*/*z*: 408.1805. Found, *m*/*z*: 430.1626 $[M+Na]^+$. $C_{24}H_{25}NNaO_5$. Calculated, *m*/*z*: 430.1625.

Diethyl 12-hexyl-2,9-dioxo-9,12-dihydro-2*H*-dipyrano-[2,3-*b*:3',2'-*h*]carbazole-3,8-dicarboxylate (DCC). Yield 25 mg (6%, two-step total yield), pale-yellow solid, mp >260.3°C (decomp.). ^{1}H NMR spectrum ($CDCl_3$), δ, ppm (*J*, Hz): 8.76 (2H, s, H Ar); 8.27 (2H, s, H Ar); 7.31 (2H, s, H Ar); 4.44 (4H, q, *J* = 7.2, $COOC\underline{H}_2CH_3$); 4.29 (2H, t, *J* = 7.2, $NC\underline{H}_2CH_2$); 1.94–1.87 (2H, m, $NCH_2C\underline{H}_2$); 1.44 (6H, t, *J* = 7.2, $COOCH_2C\underline{H}_3$); 1.39–1.25 (6H, m, $CH_2CH_2CH_2$); 0.88 (3H, t, *J* = 6.8, CH_3). ^{13}C NMR spectrum ($CDCl_3$-*d*), δ, ppm: 163.5; 157.0; 155.1; 149.7; 145.8; 121.7; 120.5, 114.6; 112.2; 96.7; 61.9; 44.3; 31.4; 28.3; 26.9; 22.5; 14.3; 14.0. Found, *m*/*z*: 532.1968 $[M+H]^+$. $C_{30}H_{30}NO_8$. Calculated, *m*/*z*: 532.1966.

Ethyl 10-hexyl-8-(hexyloxy)-2-oxo-2,10-dihydropyrano-[2,3-*b*]carbazole-3-carboxylate (HCC). Ethyl 10-hexyl-8-hydroxy-2-oxo-2,10-dihydropyrano[2,3-*b*]carbazole-3-carboxylate (**CC**) (120 mg, 0.3 mmol), anhydrous K_2CO_3

(100 mg, 0.8 mmol), KI (20 mg, 0.1 mmol), TBAB (10 mg, 0.03 mmol), and dry DMF (10 ml) were added to a three-necked flask, heated to 60°C, and stirred for 0.5 h. 1-Bromohexane (32 μl, 0.2 mmol) was dissolved in DMF (5 ml) and added to the solution dropwise. The mixture was stirred at 80°C for 2 h, and then cooled to room temperature and filtered. The filtrate was poured into ice water and stirred overnight, and the mixture was extracted with CH_2Cl_2. The solvent was removed under reduced pressure to give a gummy mass, which was purified by silica gel column chromatography, eluent petroleum ether – EtOAc, 8:1. Yield 130 mg (90%), yellow solid, mp 164.4–165.1°C. ^{1}H NMR spectrum ($CDCl_3$), δ, ppm (*J*, Hz): 8.73 (1H, s, H Ar); 8.08 (1H, s, H Ar); 7.93 (1H, d, *J* = 8.8, H Ar); 7.19 (1H, s, H Ar); 6.91 (1H, dd, *J*= 8.4, *J* = 2.0, H Ar); 6.87 (1H, d, *J* = 2.0, H Ar); 4.43 (2H, q, *J* = 7.2, $COOC\underline{H}_2CH_3$); 4.20 (2H, t, *J* = 7.2, $NC\underline{H}_2CH_2$); 4.09 (2H, t, *J* = 6.8, $OC\underline{H}_2CH_2$); 1.90–1.82 (4H, m, $OCH_2C\underline{H}_2$, $NCH_2C\underline{H}_2$); 1.43 (3H, t, *J* = 7.2, $COOCH_2C\underline{H}_3$); 1.40–1.25 (12H, m, $CH_2CH_2CH_2$); 0.93 (3H, t, *J* = 6.8, CH_3); 0.87 (3H, t, *J* = 6.8, CH_3). ^{13}C NMR spectrum ($CDCl_3$-*d*), δ, ppm: 163.9; 159.6; 157.9; 153.9; 150.5; 145.0; 143.3; 121.8; 121.4; 120.2; 115.7; 112.7; 111.0; 108.9; 95.3; 95.0; 68.6; 61.6; 43.6; 31.6; 31.5; 29.3; 28.4; 26.9; 25.8; 22.6; 22.5; 14.4; 14.1; 14.0. Found *m*/*z*: 492.2740 $[M+H]^+$. $C_{30}H_{38}NO_5$. Calculated, *m*/*z*: 492.2744. Found, *m*/*z*: 514.2565 $[M+Na]^+$. $C_{30}H_{37}NNaO_5$. Calculated, *m*/*z*: 514.2564.

Supplementary information file containing the ^{1}H, ^{13}C NMR and ESI-HRMS spectra of intermediates and target compounds (Figs. S1–S15) is available at the journal website at http://link.springer.com/journal/10593.

We gratefully acknowledge the financial support from the Science Foundation of North University of China (No. 110121).

References

1. Li, G.; Song, X.; Yu, H.; Hu, C.; Liu, M.; Cai, J.; Zhao, L.; Chen, Y.; Yang, P. *Sens. Actuators*, *B* **2018**, *259*, 177.
2. Sun, J.; Sun, J.; Mi, W.; Xue, P.; Zhao, J.; Zhai, L.; Lu, R. *Dyes Pigm.* **2017**, *136*, 633.
3. Mi, W.; Qu, Z.; Sun, J.; Sun, J.; Zhang, F.; Ye, K. *Dyes Pigm.* **2018**, *150*, 207.
4. Baran, A.; Plotniece, A.; Sobolev, A.; Vigante, B.; Gosteva, M.; Olkhovik, V. *Chem. Heterocycl. Compd.* **2012**, *48*, 287. [*Khim. Geterotsikl. Soedin.* **2012**, 305.]
5. Deng, J.; Chen, J.; Tao, Q.; Yan, D.; Fu, Y.; Tan, H. *Tetrahedron* **2018**, *74*, 3989.
6. Benhattab, S.; Cho, A.-N.; Nakar, R.; Berton, N.; François, T.-V.; Park, N.-G.; Schmaltz, B. *Org. Electron.* **2018**, *56*, 27.
7. Jiang, H.; Zhang, W.-J.; Li, P.-H.; Wang, J; Dong, C.-Z., Zhang, K.; Chen, H.-X.; Du, Z.-Y. *Bioorg. Med. Chem. Lett.* **2018**, *28*, 1320.
8. Huang, L.; Feng, Z.-L.; Wang, Y.-T.; Lin, L.-G. *Chin. J. Nat. Med.* **2017**, *15*, 881.
9. Yin, J.; He, Y.; Wang, G. *Chem. Heterocycl. Compd.* **2018**, *54*, 146. [*Khim. Geterotsikl. Soedin.* **2018**, *54*, 146.]
10. Song, H.; Zhang, J.; Wang, X.; Zhou, Y.; Xu, C.; Pang, X.; Peng, X. *Sens. Actuators*, *B* **2018**, *259*, 233.
11. Gusain, A.; Joshi, N. J.; Varde, P. V.; Aswal, D. K. *Sens. Actuators*, *B* **2017**, *239*, 734.
12. Zhu, Q.; Xiong, W.; Gong, Y.; Zheng, Y.; Che, Y.; Zhao, J. *Anal. Chem.* **2017**, *89*(22), 11908.
13. Verbitskiy, E. V.; Slepukhin, P. A.; Subbotina,Y. O.; Valova, M. S.; Schepochkin, A. V.; Cheprakova, E. M.; Rusinov, G. L.; Charushin, V. N. *Chem. Heterocycl. Compd.* **2014**, *50*, 814. [*Khim. Geterotsikl. Soedin.* **2014**, 883.]
14. Rajeshirke, M.; Sekar, N. *Opt. Mater.* **2018**, *76*, 191.
15. Bélières, M.; Sartor, V.; Fabre, P.-L.; Poteau, R.; Bordeau, G.; Chouini-Lalanne, N. *Dyes Pigm.* **2018**, *153*, 275.
16. Bhagwat, A. A.; Mohbiya, D. R.; Avhad, K. C.; Sekar, N. *Spectrochim. Acta*, *Part A* **2018**, *203*, 244.
17. Li, T.; Gao, J.; Cui, Y.; Zhong, C. J.; Ye, Q.; Han, L. *J. Photochem. Photobiol.*, *A* **2015**, *303–304*, 91.
18. Lu, T.-F.; Li, W.; Zhang, H.-X. *Org. Electron.* **2018**, *59*, 131.
19. Liu, D.; Cao, Y.; Yan, X.; Wang, B. *Res. Chem. Intermed.* **2019**, *45*, 2429.
20. Jin, F.; Rong, Z.; Guo, X.; Ma, M.; Lv, J.; Zhang, L.; Liao, R.; Liu Y.; Tao, D.; Tian, Y. *Dyes Pigm.* **2018**, *150*, 174.
21. Sharma, N.; Kumar, S.; Chandrasekaran, Y.; Satish, P. *Org. Electron.* **2016**, *38*, 180.
22. Cai, Z.-B.; Liu, S.-S.; Li, B; Dong, Q.-J.; Liu, Z.-L.; Zheng, M.; Li, S.-L.; Tian, Y.-P.; Chen, L.-J.; Ye, Q. *Dyes Pigm.* **2019**, *165*, 200.
23. Naik, P.; Su, R.; Elmorsy, M. R.; El-Shafei, A.; Adhikari, A. V. *Photochem. Photobiol. Sci.* **2018**, *17*, 302.
24. Nabavi, S. M. J.; Hosseinzadeh, B.; Tajbakhsh, M.; Alinezhad, H. *J. Mater. Sci.: Mater. Electron.* **2018**, *29*, 3270.
25. Chen, S.; Zheng, Y.-C.; Zheng, M.-L.; Dong, X.-Z.; Jin, F.; Zhao, Z.-S.; Duan, X.-M. *J. Mater. Chem. C* **2017**, *5*, 470.
26. Xie, P.; Yuan, N.; Li, S.; Ouyang, Y.; Zhu, Y.; Liang, H. *Luminescence* **2018**, *33*, 604.
27. Yang, L.; Zhu, W.; Fang, M.; Zhang, Q; Li, C. *Spectrochim. Acta*, *Part A* **2013**, *109*, 186.
28. Yin, J.; Bing, Q. J.; Wang, L.; Wang, G. *Spectrochim. Acta*, *Part A* **2018**, *189*, 495.
29. Sathiyan, G.; Sakthivel, P. *Dyes Pigm.* **2017**, *143*, 444.
30. Panthi, K., Adhikari, R. M., Kinstle, T. H. *J. Phys. Chem. A* **2010**, *114*, 4550.
31. Wang, S.; Yu, C.; Choi, M.-S.; Kim, S.-H. *J. Photochem. Photobiol.*, *A* **2007**, *192*, 17.
32. Jeong, J.; Rao, B. A.; Son, Y.-A. *Sens. Actuators*, *B* **2015**, *220*, 1254.
33. Sengul, I. F.; Okutan, E.; Kandemir, H.; Astarcı, E.; Çoşut, B. *Dyes Pigm.* **2015**, *123*, 32.
34. Eçik, E. T.; Özcan, E.; Kandemir, H.; Sengul, I. F.; Çoşut, B. *Dyes Pigm.* **2017**, *136*, 441.
35. Yu, T.; Zhu, Z.; Bao, Y.; Zhao, Y.; Liu, X.; Zhang, H. *Dyes Pigm.* **2017**, *147*, 260.
36. Azaza, N. B.; Elleuch, S.; Khemakhem, S.; Abid, Y.; Ammar, H. *Opt. Mater.* **2018**, *83*, 138.
37. Yang, X.; Jing, L.; Chen, Z. *Chem. Heterocycl. Compd*, **2018**, *54*, 1065. [*Khim. Geterotsikl. Soedin.* **2018**, *54*, 1065.]
38. Rong, L.; Liu, Q.; Tang, J.; Chi, Z. *Heterocycles* **2010**, *81*, 977.